

1 **A Mixed-Penalty Biphasic Finite Element Formulation**
2 **Incorporating Viscous Fluids and Material Interfaces**
3

4 B. Chan^{1,3}, P. S. Donzelli^{2,3} and R. L. Spilker^{1,2,3}
5

6 ¹Department of Mechanical Engineering, Aeronautical Engineering, and Mechanics
7

8 ²Department of Biomedical Engineering
9

10 ³Scientific Computation Research Center
11

12 Rensselaer Polytechnic Institute
13

14 Troy, New York 12180

15 Running title:

16 Biphasic Interface FEM

17 Corresponding author:

18 R. L. Spilker

19 Department of Biomedical Engineering

20 JEC 7049

21 Rensselaer Polytechnic Institute

Troy, NY 12180-3590

(518) 276 2154 (phone)

(518) 276 3035 (fax)

spilker@rpi.edu

1 Abstract - The fluid viscosity term of the fluid phase constitutive equation and the interface
2 boundary conditions between biphasic, solid and fluid domains have been incorporated into a
3 mixed-penalty finite element formulation of the linear biphasic theory for hydrated soft tissue. The
4 finite element code can now model a single-phase viscous incompressible fluid, or a single-phase
5 elastic solid, as limiting cases of a biphasic material. Interface boundary conditions allow the
6 solution of problems involving combinations of biphasic, fluid and solid regions. To incorporate
7 these conditions, the volume-weighted mixture velocity is introduced as a degree of freedom at
8 interface nodes, so that the kinematic continuity conditions are satisfied by conventional finite
9 element assembly techniques. Results comparing our numerical method with an independent,
10 analytic solution for the problem of Couette flow over rigid and deformable porous biphasic layers
11 show that the finite element code accurately predicts the viscous fluid flows and deformation in the
12 porous biphasic region. Thus, the analysis can be used to model the interface between synovial
13 fluid and articular cartilage in diarthrodial joints. This is an important step toward modeling and
14 understanding the mechanisms of joint lubrication and another step toward fully modeling the *in*
15 *vivo* behavior of a diarthrodial joint.

16 **Keywords** -- biphasic finite element formulation, fluid viscosity, material interface, Couette
17 flow

INTRODUCTION

The biomechanics of diarthrodial joints has been and continues to be of great interest to researchers. It is believed that a better comprehension of the friction, lubrication and wear of diarthrodial joints will lead to a better understanding of the pathogenesis of osteoarthritis ^{7, 15, 18}. The two materials common to all diarthrodial joints are articular cartilage (a porous, permeable, viscoelastic, multi-phase material) and synovial fluid (a non-Newtonian fluid) ¹⁷. Thus, changes in the mechanical properties of articular cartilage or the rheological properties of synovial fluid may lead to increase friction and wear within the joints, leading to degenerative joint disorders, such as osteoarthritis ¹.

Since interstitial fluid flow plays an important role in the deformational behavior of articular cartilage, a realistic model of cartilage must incorporate the fluid component as a distinct phase of the system within the tissue. Mow and co-workers ¹⁷ have developed a biphasic continuum model that can accurately represent the deformational behavior of hydrated soft tissue such as articular cartilage or meniscus in the human knee joint. In order to solve the governing biphasic equations for realistic joint mechanics problems with complex geometry and boundary conditions, numerical methods, such as the finite element method, must be used. Various finite element formulations of the biphasic theory have been developed corresponding to the linear biphasic theory ^{19, 20, 25}, the nonlinear biphasic theory including strain-dependent permeability ²¹ and finite deformation theories ^{22, 23}. However, these formulations consider only the biphasic soft tissue and do not include the dynamic interaction between the articular cartilage and its surrounding fluid.

Understanding the modes of diarthrodial joint lubrication requires an analysis incorporating both the soft tissues and the synovial fluid, including proper formulation of the boundary conditions at the interface between articular cartilage and synovial fluid. In the context of the biphasic theory, Hou *et al.* ¹⁰ have derived the boundary conditions at the interface between a viscous fluid and a biphasic material. In Hou's study, single-phase continua such as solid or fluid

1 are modeled as a mixture with only one phase. Thus the interfacial conditions derived for the
 2 mixture theory are also applicable to the boundary between mixtures and single-phase continua.
 3 These boundary conditions are derived from balances of mass, momentum and energy and must be
 4 consistent with the imposed kinematic boundary conditions. In addition, the imposed kinematic
 5 boundary conditions must reduce to the kinematic conditions in single phase continuum mechanics
 6 when mixtures reduce to single phase continua.

7 While biphasic contact finite element formulations ⁶ and analytic contact solutions ^{3, 4} do
 8 exist, these do not account for fluid viscosity. Few studies have used numerical investigations to
 9 understand the importance of synovial fluid in joint lubrication, for example ^{8, 9, 12, 24}. In the
 10 present study, both fluid viscosity and the boundary conditions at the cartilage-synovial fluid
 11 interface ¹⁰ will be incorporated into the mixed-penalty finite element formulation ¹⁹ of the linear
 12 biphasic theory. This will be done by introducing a volume-weighted mixture velocity as a degree
 13 of freedom at the interface nodes. With proper treatment of the constraints and the assembly of
 14 elements, the interface kinematic boundary conditions are satisfied exactly in the finite element
 15 solution. We will then investigate problems that involve solid, fluid, and biphasic regions.

16 **LINEAR BIPHASIC THEORY WITH VISCOUS FLUID**

17 In this study, viscosity is added to the fluid phase of the linear biphasic theory so that
 18 single phase continua can be treated as limiting cases in which the solid or fluid content is zero.
 19 The subchondral bone will be modeled as an elastic solid and the synovial fluid as a viscous fluid.
 20 In the linear biphasic model, the phases are assumed to be immiscible, incompressible and to
 21 undergo small deformations. The governing differential equations of the linear biphasic model
 22 with a viscous, incompressible fluid for a material domain Ω having volume V with boundary
 23 Γ are (in tensor form) ¹⁷:

$$24 \quad \nabla \cdot (\phi^s \mathbf{v}^s + \phi^f \mathbf{v}^f) = 0 \quad (1)$$

$$25 \quad \nabla \cdot \boldsymbol{\sigma}^\alpha + \boldsymbol{\Pi}^\alpha = \mathbf{0}, \quad \alpha = s, f \quad (2)$$

$$1 \quad \boldsymbol{\sigma}^s = -\phi^s p \mathbf{I} + \mathbf{C}^s \boldsymbol{\epsilon}^s \quad (3)$$

$$2 \quad \boldsymbol{\sigma}^f = -\phi^f p \mathbf{I} + \mathbf{C}^f \dot{\boldsymbol{\epsilon}}^f \quad (4)$$

$$3 \quad \boldsymbol{\Pi}^s = -\boldsymbol{\Pi}^f = K(\mathbf{v}^f - \mathbf{v}^s). \quad (5)$$

4 They correspond to the continuity equation for the mixture (1), momentum equations for each
5 phase (2), constitutive equations (3),(4) and the diffusive drag force (5). The superscripts 'f' and
6 's' denote quantities associated with the fluid and solid phases respectively, ϕ^s and ϕ^f are volume
7 fractions which sum to unity, \mathbf{v} is the velocity vector, $\boldsymbol{\sigma}$ is the Cauchy stress tensor, \mathbf{C}^α are the
8 fourth-rank tensors of material coefficients, $\boldsymbol{\Pi}$ is the diffusive momentum exchange between the
9 two phases, p is the apparent pressure, $\boldsymbol{\epsilon}$ is the infinitesimal strain tensor, $\dot{\boldsymbol{\epsilon}}$ is the rate of
10 deformation tensor and K is the diffusive drag coefficient ¹⁴:

$$11 \quad K = \frac{\phi^{f^2}}{\kappa}, \quad (6)$$

12 with κ the tissue permeability constant. Note that \mathbf{C}^s has only two independent terms for the
13 linear, isotropic solid phase, and \mathbf{C}^f will have only the fluid viscosity term, μ^f , multiplying the rate
14 of deformation, for the viscous, incompressible, Newtonian fluid considered here. Boundary
15 conditions on solid displacements, fluid velocities, solid traction and fluid traction are required on
16 the surfaces Γ^{u^s} , Γ^{u^f} , Γ^{σ^s} and Γ^{σ^f} , respectively. To complete the problem definition the
17 appropriate initial conditions must also be specified; these will be specified in the context of each
18 example problem. From the above equations the finite element formulation of the linear biphasic
19 theory with a viscous fluid can now be developed.

20 **FINITE ELEMENT FORMULATION**

21 *Mixed-Penalty Formulation*

22 The mixed-penalty formulation of Spilker and Maxian ^{16, 19} for the linear biphasic theory
23 is extended here to allow for viscosity in the fluid phase of the biphasic material. Most details of

1 the formulation are omitted here since they are similar to the derivation without viscosity 5, 16, 19.

2 In the mixed-penalty formulation, the continuity equation is replaced by the penalty form,

$$3 \quad \nabla \cdot (\phi^s \mathbf{v}^s + \phi^f \mathbf{v}^f) + \frac{p}{\beta} = 0, \quad (7)$$

4 where β is a user-defined penalty number. In the Galerkin weighted residual method, this penalty
 5 form of the continuity equation, the momentum equations and natural boundary conditions are then
 6 each multiplied by an appropriate weighting function, integrated over the domain, summed together
 7 and equated to zero

$$8 \quad \int_{\Omega} w^c \left[\nabla \cdot (\phi^s \mathbf{v}^s + \phi^f \mathbf{v}^f) + \frac{p}{\beta} \right] d\Omega +$$

$$\int_{\Omega} \mathbf{w}^s (\nabla \cdot \boldsymbol{\sigma}^s + \Pi^s) d\Omega + \int_{\Omega} \mathbf{w}^f (\nabla \cdot \boldsymbol{\sigma}^f + \Pi^f) d\Omega + \quad (8)$$

$$\int_{\Gamma^{\sigma^s}} \mathbf{h}^s (\boldsymbol{\sigma}^s \mathbf{n} - \bar{\mathbf{t}}^s) d\Gamma + \int_{\Gamma^{\sigma^f}} \mathbf{h}^f (\boldsymbol{\sigma}^f \mathbf{n} - \bar{\mathbf{t}}^f) d\Gamma = 0$$

9 Equations (3) through (6) are substituted into the weighted residual, Eq. (8), and the divergence
 10 theorem is applied to the terms containing derivatives of stress. By proper manipulation the weak
 11 form of the weighted residual is obtained, after which the finite element discretization can be
 12 applied. This weak form contains solid displacement, solid velocity, fluid velocity and pressure as
 13 independent field variables. To guarantee that all the integrals in the weak form remain finite, the
 14 solid and fluid velocities/displacements are assumed to be C^0 continuous, while the pressure is
 15 allowed to be discontinuous between elements.

16 The field variables are interpolated within the element in terms of a corresponding set of
 17 nodal values in the following form:

$$18 \quad \mathbf{u}^s = \mathbf{N}^s \mathbf{d}^{es}, \quad \mathbf{v}^s = \mathbf{N}^s \mathbf{v}^{es}, \quad \mathbf{v}^f = \mathbf{N}^f \mathbf{v}^{ef}, \quad p = \mathbf{N}_p \mathbf{p}^e, \quad (9)$$

19 where \mathbf{d}^{es} , \mathbf{v}^{es} and \mathbf{v}^{ef} are the nodal solid displacements, nodal solid velocities and nodal fluid
 20 velocities for a typical element 'e' and \mathbf{p}^e is the vector of coefficients of the the pressure

1 interpolation for an element. In general, the interpolation functions used for the solid and fluid
 2 phases are the same, so we set $\mathbf{N}^s = \mathbf{N}^f = \mathbf{N}$. Since this is a Galerkin approximation, the
 3 interpolation used for the weighting functions are the same as those used for the field variables,
 4 with \mathbf{w}^{es} , \mathbf{w}^{ef} and \mathbf{w}^{ec} as arbitrary coefficients for element 'e'. For a finite element program, the
 5 stress and strain tensors are represented as vectors, and the corresponding fourth-rank tensors of
 6 material coefficients are represented as square matrices. In this reduced index form, the matrix \mathbf{B}
 7 will represent the symmetric gradient operation on the spatial interpolation, \mathbf{N} , and the vector \mathbf{m}
 8 will be the representation of the Kronecker delta.

9 The element interpolations are substituted into the weak form of the weighted residual,
 10 producing the following set of matrix equations:

$$\begin{aligned}
 & \sum_e \begin{Bmatrix} \mathbf{w}^{esT} \\ \mathbf{w}^{efT} \\ \mathbf{w}^{ecT} \end{Bmatrix} \begin{bmatrix} \mathbf{c} & -\mathbf{c} & \mathbf{0} \\ -\mathbf{c} & \mathbf{c} + \mathbf{k}^{ef} & \mathbf{0} \\ -\phi^s \mathbf{a}^T & -\phi^f \mathbf{a}^T & \mathbf{0} \end{bmatrix} \begin{Bmatrix} \mathbf{v}^{es} \\ \mathbf{v}^{ef} \\ \mathbf{0} \end{Bmatrix} + \\
 11 & \sum_e \begin{Bmatrix} \mathbf{w}^{esT} \\ \mathbf{w}^{efT} \\ \mathbf{w}^{ecT} \end{Bmatrix} \begin{bmatrix} \mathbf{k}^{es} & \mathbf{0} & -\phi^s \mathbf{a} \\ \mathbf{0} & \mathbf{0} & -\phi^f \mathbf{a} \\ \mathbf{0} & \mathbf{0} & \frac{1}{\beta} \mathbf{k}_p \end{bmatrix} \begin{Bmatrix} \mathbf{d}^{es} \\ \mathbf{0} \\ \mathbf{p}^e \end{Bmatrix} = \sum_e \begin{Bmatrix} \mathbf{w}^{esT} \\ \mathbf{w}^{efT} \\ \mathbf{w}^{ecT} \end{Bmatrix} \begin{Bmatrix} \mathbf{f}^{es} \\ \mathbf{f}^{ef} \\ \mathbf{0} \end{Bmatrix}, \tag{10}
 \end{aligned}$$

12 where the element submatrices are defined as:

$$\mathbf{a} = \int_{\Omega_e} (\mathbf{m}\mathbf{B})^T \mathbf{N}_p d\Omega \tag{11}$$

$$\mathbf{k}^{e\alpha} = \int_{\Omega_e} \mathbf{B}^T \mathbf{C}^\alpha \mathbf{B} d\Omega, \quad \alpha = s, f \tag{12}$$

$$\mathbf{c} = \int_{\Omega_e} \mathbf{K} \mathbf{N}^T \mathbf{N} d\Omega \tag{13}$$

$$\mathbf{k}_p = \int_{\Omega_e} \mathbf{N}_p^T \mathbf{N}_p d\Omega, \tag{14}$$

17 and all other terms are as defined before. The current formulation differs from the original mixed-
 18 penalty formulation ¹⁶ by the addition of the fluid stiffness term, \mathbf{k}^{ef} .

19 Because pressure is discontinuous between elements, the pressure coefficients, \mathbf{p}^e , can be

1 eliminated at the element level by using the last equation in matrix equation (10). This produces the
 2 final set of matrix equations for the mixed-penalty formulation:

$$\begin{aligned}
 & \sum_e \begin{Bmatrix} \mathbf{w}^{es^T} \\ \mathbf{w}^{ef^T} \end{Bmatrix} \left\{ \beta \begin{bmatrix} \phi^{s^2} \mathbf{A} & \phi^s \phi^f \mathbf{A} \\ \phi^s \phi^f \mathbf{A} & \phi^{f^2} \mathbf{A} \end{bmatrix} + \begin{bmatrix} \mathbf{c} & -\mathbf{c} \\ -\mathbf{c} & \mathbf{c} + \mathbf{k}^{ef} \end{bmatrix} \right\} \begin{Bmatrix} \mathbf{v}^{es} \\ \mathbf{v}^{ef} \end{Bmatrix} + \\
 & \sum_e \begin{Bmatrix} \mathbf{w}^{es^T} \\ \mathbf{w}^{ef^T} \end{Bmatrix} \begin{bmatrix} \mathbf{k}^{es} & \mathbf{0} \\ \mathbf{0} & \mathbf{0} \end{bmatrix} \begin{Bmatrix} \mathbf{d}^{es} \\ \mathbf{0} \end{Bmatrix} = \sum_e \begin{Bmatrix} \mathbf{w}^{es^T} \\ \mathbf{w}^{ef^T} \end{Bmatrix} \begin{Bmatrix} \mathbf{f}^{es} \\ \mathbf{f}^{ef} \end{Bmatrix} \quad , \tag{15}
 \end{aligned}$$

3 where $\mathbf{A} = \mathbf{a} \mathbf{k}_p^{-1} \mathbf{a}^T$.

4 The element matrices are then assembled into their respective global matrices by the
 5 standard Boolean assembly operator. Then, for arbitrary weighting functions, the assembled
 6 coefficients of the weighting functions must be nonzero and the mixed-penalty formulation of the
 7 linear biphasic theory with viscous fluid produces the following system of first order differential
 8 equations,
 9

$$\mathbf{C} \mathbf{v} + \mathbf{K} \mathbf{d} = \mathbf{F}, \tag{16}$$

10 where \mathbf{C} includes the penalty terms, diffusive drag and fluid viscosity, and \mathbf{K} is the assembled
 11 counterpart of the block two-by-two element stiffness matrix. The vectors \mathbf{d} and \mathbf{v} are the
 12 assembled degree of freedom vectors and \mathbf{F} is the assembled force vector. At the global level, the
 13 ordering of the degrees of freedom in \mathbf{d} and \mathbf{v} are different from the ordering at the element level.
 14 For computational efficiency when performing element integrals, the degrees of freedom at the
 15 element level are ordered as all solid degrees of freedom followed by all fluid degrees of freedom.
 16 At the global level, the degrees of freedom are ordered alternately as solid and fluid degrees of
 17 freedom for each node.
 18

Solution of the System of Equations

The system of equations in Eq. (16) is solved using finite difference techniques. Given times t_{m+1} and t_m separated by a time increment $\Delta t = t_{m+1} - t_m$, the system of equations at time t_{m+1} is solved using the generalized trapezoidal family of first order finite difference rules¹¹.

$$\begin{aligned} \mathbf{d}_{m+1} &= \mathbf{d}_m + \Delta t \mathbf{v}_{m+\omega} \\ \mathbf{v}_{m+\omega} &= (1-\omega)\mathbf{v}_m + \omega\mathbf{v}_{m+1}, \quad \omega \in [0,1] \end{aligned} \quad (17)$$

Writing Eq. (16) at $t=t_{m+1}$ and substituting from Eq. (17) yields the following set of matrix equations to be solved at each time step:

$$(\mathbf{C} + \omega\Delta t\mathbf{K})\mathbf{v}_{m+1} = \mathbf{F}_{m+1} - \mathbf{K}(\mathbf{d}_m + (1-\omega)\Delta t\mathbf{v}_m). \quad (18)$$

Once a set of initial conditions is given, this set of equations can be solved recursively. In our study, an unconditionally stable implicit rule ($\omega \geq 1/2$) is used²¹.

Selection of Penalty Number

The penalty term, β , is a user-defined number that should be large enough to enforce constraint conditions yet not so large that the solution of the governing equations become ill-conditioned. Through earlier investigations on penalty formulations of the linear biphasic theory²¹, and extensions for a viscous fluid phase, we choose the penalty term according to the following guideline :

$$\beta = ct_0 \frac{\lambda^s + 2\mu^s}{\phi^s} + c \frac{\mu^f}{\phi^s}, \quad (19)$$

where t_0 is a reference time (*e.g.* ramp time), c is a computer-dependent parameter related to the accuracy of the numerical calculations (c is usually chosen in the range 10^7 to 10^9), λ and μ are the solid phase Lamé parameters and μ^f is the viscosity of the fluid. Recognize that for parameters representative of articular cartilage, the second term above can be neglected. It has been observed that variations in β by ± 2 orders of magnitude have negligible affect on the solution.

1 In the limiting case of a single phase fluid, however, the penalty number is chosen
 2 according to the criteria established for penalty solutions of viscous incompressible flows ¹¹:

$$3 \quad \beta = c\mu^f, \quad (20)$$

4 where μ^f and c are as described above.

5 FINITE ELEMENT FORMULATION OF THE INTERFACE 6 BOUNDARY CONDITIONS

7 The development of the interface boundary conditions can be found in Hou *et al.* ¹⁰. Since
 8 both the solid and fluid phases for the biphasic mixture are intrinsically incompressible, the jump
 9 condition for the mass across a surface of discontinuity is

$$10 \quad [[\phi^s \mathbf{v}^s + \phi^f \mathbf{v}^f]] \cdot \mathbf{n} = 0, \quad (21)$$

11 where $[[()]]$ represents the jump in quantity $()$, \mathbf{n} is the normal to the surface of discontinuity and
 12 the argument here is the volume-weighted mixture velocity. In order to account for the viscous
 13 interactions at the interface, an additional kinematic boundary condition has to be imposed. For
 14 viscous fluids, the "no-slip" condition at the fluid/solid interface must be specified. Under
 15 ordinary circumstances, viscous fluids adhere to solid (non-porous) surfaces, such that

$$16 \quad \lim_{\mathbf{x} \rightarrow \mathbf{x}_s} \mathbf{v}^f(\mathbf{x}) = \mathbf{v}_{surface}(\mathbf{x}_s), \quad (22)$$

17 where \mathbf{x}_s is the coordinate for the surface and $\mathbf{v}_{surface}$ is the velocity of the surface. Since a single-
 18 phase material is treated as a special case of a biphasic medium, it is proposed that all kinematic
 19 boundary conditions at a surface of discontinuity within a biphasic material reduce, in the limiting
 20 case of $\phi^f \rightarrow 0$ on one side of the surface and $\phi^s \rightarrow 0$ on the other side, to the condition described in
 21 Eq. (22).

22 The following jump condition satisfies the above condition:

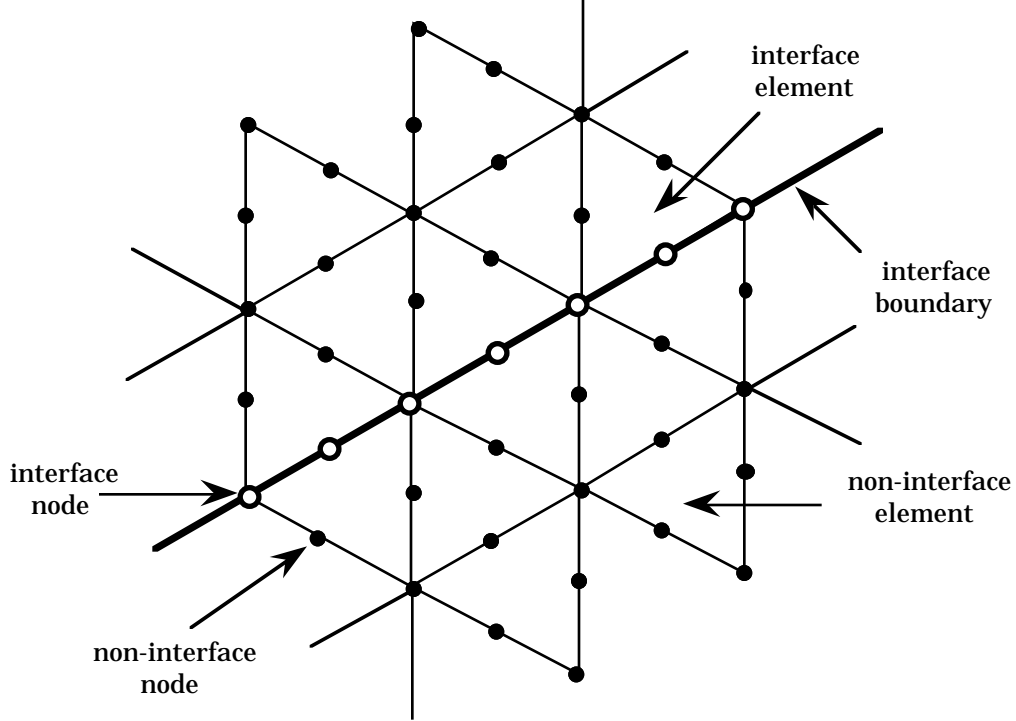
$$23 \quad [[\tilde{\phi}^s \mathbf{v}^s + \tilde{\phi}^f \mathbf{v}^f]] \cdot \boldsymbol{\tau} = 0, \quad (23)$$

1 where $\tilde{\phi}^s$ and $\tilde{\phi}^f$ are the surface area fraction of the solid and fluid phases respectively, and $\boldsymbol{\tau}$ is
2 any tangent vector of the surface. Since the pore structure of articular cartilage is assumed to be
3 isotropic, the area fractions can be shown to be equivalent to the volume fractions. The jump
4 condition in Eq. (23) is called a "pseudo-no-slip" boundary condition because it allows the solid
5 and fluid phases to have different velocities at the interface. Combining Eqns. (21),(23), a single
6 vector equation for the volume-weighted mixture velocity is obtained:

$$7 \quad \left[\left[\phi^s \mathbf{v}^s + \phi^f \mathbf{v}^f \right] \right] = \mathbf{0}. \quad (24)$$

8 We now consider the choice of element degrees of freedom that will facilitate the
9 enforcement of the interface continuity conditions. The nodal degrees of freedom for an element
10 have been defined as containing first the solid degrees of freedom for all nodes in the element, then
11 the fluid degrees of freedom. The traditional assembly of these degrees of freedom along an
12 interface would satisfy continuity of velocity, but would not satisfy the interface conditions
13 between two dissimilar materials. By equating the solid nodal velocities at the interface, the
14 condition that the solid velocities be continuous across a discontinuity (interface) is properly
15 satisfied. However, the fluid velocity across a discontinuity need not be continuous, and thus the
16 standard biphasic finite element analysis will impose an incorrect interface condition. In what
17 follows, we define a method for properly accounting for the interface boundary conditions.

18 Figure 1 shows a section of a finite element mesh at an interface. Some of the terms that
19 will be used in the discussion that follows are defined in this figure. Note that an interface element
20 is an element that contains at least one interface node.



1
2 Figure 1. Portion of an arbitrary finite element mesh at an interface between two dissimilar
3 materials. An interface element is one which contains at least one interface node. For the
4 present formulation, we employ a quadratic, six-node velocity interpolation and a linear,
5 discontinuous pressure interpolation. The pressure interpolation is not directly affected by
6 our interface methodology, and is not shown.

7 For purposes of this discussion the degrees of freedom for an element are reordered to
8 contain the solid degrees of freedom for the first node, then the second, and so on, followed by a
9 similar collection of the fluid degrees of freedom. At a node, the solid or fluid degrees of freedom
10 are ordered according to the basis vectors, either $\{x,y\}$ or $\{r,z\}$ for the two dimensional case.

11 Thus, the degrees of freedom for node 'a' of element 'e' are

$$12 \quad \mathbf{v}_a^e = \begin{Bmatrix} \mathbf{v}_a^{es} \\ \mathbf{v}_a^{ef} \end{Bmatrix}. \quad (25)$$

13 In order to satisfy the kinematic jump condition in Eq. (24), the volume-weighted mixture
14 velocity is introduced as a degree of freedom for nodes at an interface, replacing the fluid phase
15 velocity degree of freedom. The degrees of freedom at the interface nodes become

$$16 \quad \mathbf{v}_a^{e*} = \begin{Bmatrix} \mathbf{v}_a^{es} \\ \phi^s \mathbf{v}_a^{es} + \phi^f \mathbf{v}_a^{ef} \end{Bmatrix}. \quad (26)$$

$$\begin{aligned}
& \mathbf{T}_a^{ss} = \mathbf{I}, \quad \mathbf{T}_a^{sf} = \mathbf{0} \\
1 \quad \mathbf{T}_a^{fs} &= \begin{bmatrix} -\frac{\phi^s}{\phi^f} & 0 \\ 0 & -\frac{\phi^s}{\phi^f} \end{bmatrix}, \quad \mathbf{T}_a^{ff} = \begin{bmatrix} \frac{1}{\phi^f} & 0 \\ 0 & \frac{1}{\phi^f} \end{bmatrix}. \tag{30}
\end{aligned}$$

2 For a single phase fluid region no contribution comes from the solid terms. In order to eliminate
3 the solid contributions at fluid interface nodes all of the submatrices will be null except for the \mathbf{T}^{ff}
4 terms, which will be identities. For a single phase solid region the \mathbf{T}^{ss} terms will be identities, and
5 the remainder will be null. With the interface element matrices transformed, their contributions
6 must be properly assembled into the global matrices and the appropriate constraints applied in order
7 to satisfy the interface boundary conditions in Eq. (24), which includes the "pseudo-no-slip"
8 condition.

9 When transformed interface degrees of freedom from the local nodes of two different
10 elements are assembled into their global positions, special considerations are still necessary. For
11 non-interface nodes on an interface element, or interface nodes between two dissimilar biphasic
12 materials, the local contributions simply go to the corresponding global locations. For an interface
13 between a biphasic material and a single-phase fluid, the contributions still go to the standard
14 locations, but note that the fluid node is contributing zeros to the global solid degree of freedom
15 and the biphasic node contributes the weighted mixture velocity to the global fluid degree of
16 freedom. For an interface between solid and biphasic regions the solid velocities from each region
17 are assembled together into the global interface degree of freedom to satisfy the continuity of the
18 solid across the interface. The volume-weighted mixture velocity degree of freedom from the
19 biphasic element is also assembled into the global solid degree of freedom to satisfy the jump
20 condition of Eq. (24). This leaves the global fluid interface degree of freedom of this node with no
21 contributions, thus this degree of freedom must be constrained to zero at the global level. For a
22 single-phase fluid and single-phase solid interface, the no-slip condition must be also be satisfied.
23 The fluid degree of freedom from the fluid element and the solid degree of freedom from the solid

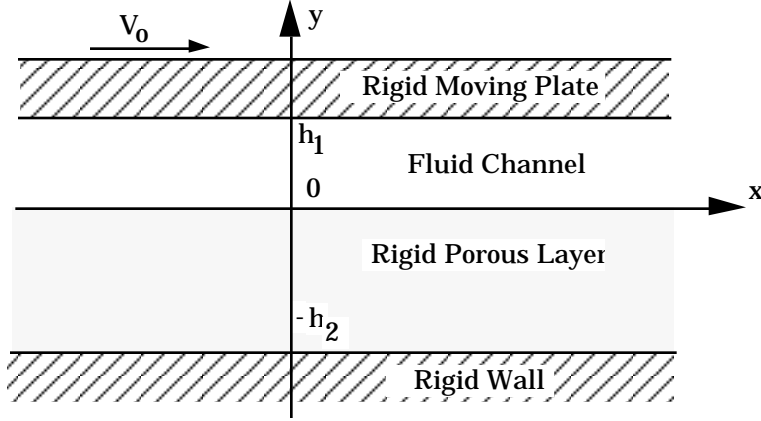
1 element are each assembled into the global solid degree of freedom. By doing this, we equate the
2 fluid velocity of the node on the fluid side of the interface with the solid velocity of the node on the
3 solid side, thus satisfying the no-slip condition and the jump condition. The global fluid interface
4 degree of freedom of this node is left with no contributions from the element level and therefore
5 must be constrained to zero.

6 For single-phase fluid and single-phase solid, additional constraints are applied. For a
7 single-phase fluid, all solid degrees of freedom that are not prescribed or on an interface are
8 constrained to zero (since there is no contribution of the solid phase in this region). Similarly, the
9 fluid degrees of freedom of a single-phase solid are also constrained to zero (since there is no
10 contribution of the fluid phase in this region) with the exception of those that are prescribed or on
11 an interface. With the interface boundary conditions implemented in this fashion, the finite element
12 code can model any combination of solid/fluid/biphasic material interfaces.

13 **EXAMPLE PROBLEMS AND RESULTS**

14 *Couette Flow over a Rigid Porous-Permeable Layer*

15 The boundary conditions derived by Hou ¹⁰ have been used in that study to formulate the
16 classical Taylor problem of Couette flow over a rigid, porous-permeable medium. In this problem,
17 the steady viscous fluid flowing over and inside the porous-permeable layer is sustained by the
18 movement of the upper boundary of the fluid layer with a speed V_0 , as illustrated in Figure 2.
19 The porous layer is assumed to be rigid and stationary and thus the velocity and displacement of
20 the porous layer are zero. The moving plate and the porous layer are also assumed to be infinite in
21 the x direction.



1
2 Figure 2. Schematic diagram of Couette flow over a porous-permeable layer. The finite
3 element model will contain only the fluid channel and rigid, porous layer. Solid velocity is
4 set to zero at all boundaries of the model. Fluid velocity is prescribed to V_0 at the top of the
5 fluid channel, and zero at the bottom of the porous layer, and is unknown at the left and
6 right edges.

7 The analytical solution of this problem states that the fluid flux depends on the following
8 flow and geometric parameters ¹⁰:

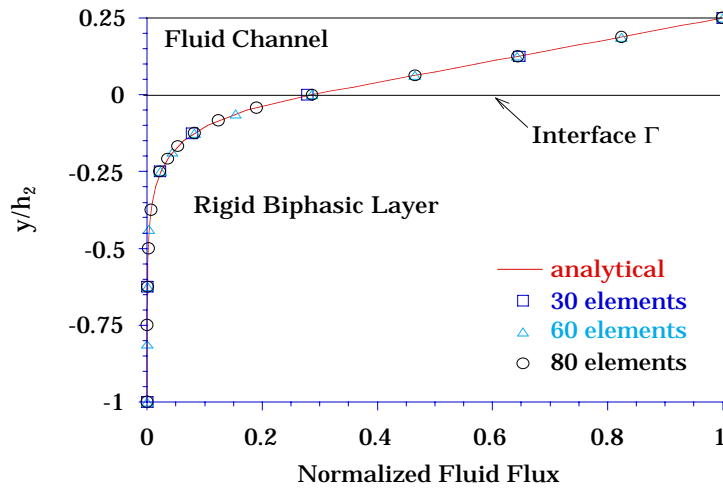
9
$$\delta = \sqrt{\frac{\mu^a}{h_2^2 K}}, \quad \xi = \frac{h_1}{h_2}, \quad \eta = \frac{\phi^{f^2} \mu^f}{\mu^a}, \quad (31)$$

10 where δ is a measure of viscous drag of the outside fluid relative to the diffusive drag of interstitial
11 fluid within the porous medium, ξ is the thickness ratio of the viscous fluid layer relative to the
12 porous solid layer and η defines a weighted viscosity ratio; μ^f is the viscosity of the fluid in the
13 channel and μ^a is the apparent viscosity of the fluid in the porous layer. For low values of δ ($<$
14 0.02), the amount of fluid flow in the porous layer is small and the boundary layer that develops at
15 the surface will be narrow. Therefore, for purposes of validating the finite element code the
16 combination of material parameters chosen will be such that δ is not too small.

17 In this problem, the rigid porous layer will be modeled as a biphasic material ($\phi^f=0.8$) with
18 high elastic modulus ($\lambda^s=1.0$ GPa, $\mu^s=3.0$ GPa); the viscous fluid will be modeled as a limiting
19 case of a biphasic material ($\phi^f=1$) with a viscosity of 1.0Ns/m² (the viscosity of synovial fluid ¹³).
20 The solid velocity is set to zero on the entire boundary, while fluid velocity is prescribed across the
21 top of the fluid layer ($y=h_1$), unknown at the left and right edges and zero at the bottom ($y=-h_2$).

1 This problem assumes the porous layer and the plate to be infinite in length, therefore the length to
 2 height ratio for the geometry must be large. Since the solid displacement is assumed to be zero,
 3 only the height of the single-phase fluid layer is taken into account in determining the length-to-
 4 height ratio. The results show that this is a valid representation of the infinite length.

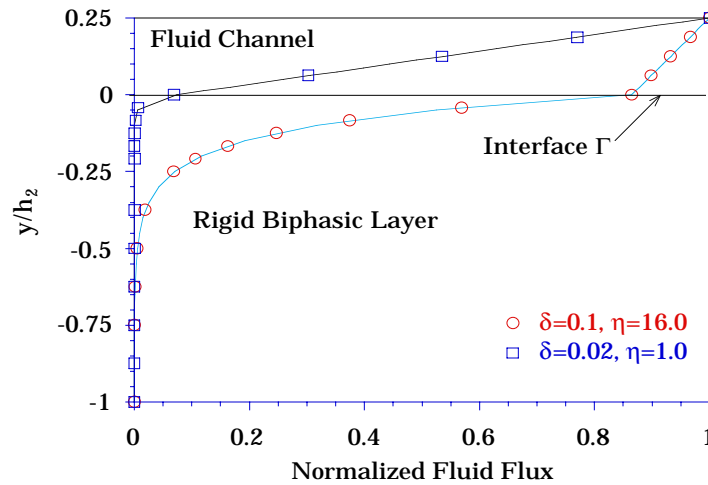
5 A finite element mesh manually graded toward the interface is used, and has been
 6 determined to produce converged solutions. Figure 3 shows the normalized fluid flux, $\phi^f v_x^f / V_0$,
 7 versus the dimensionless coordinate y/h_2 for the problem of Couette flow over a rigid porous solid
 8 with $\xi = 0.25$, $\eta = 1.0$ and $\delta = 0.1$. The results obtained for this problem show excellent
 9 agreement with the analytical solutions. Since the solid degrees of freedom in the porous solid are
 10 not constrained to zero in the finite element mesh, solid displacements are also obtained from the
 11 analysis. These calculated displacements, however, are negligible, in agreement with the
 12 assumption that the material is rigid.



13 Figure 3. Finite element solution (symbols) and analytical solution (line) of the fluid flux
 14 profile in the fluid channel and in the rigid porous layer (corresponding to Figure 2) with η
 15 = 1 and $\delta = 0.1$.
 16

17 Figure 4 show the finite element analyses and analytical solutions for two other cases.
 18 Though the material parameters for these cases may not model any particular material, the results

1 are instructive in that they show that the finite element code is valid for a wide range of parameters.
 2 The first case, with $\eta=16.0$ and $\delta=0.1$, shows that even for a large continuous change in fluid flux
 3 across the interface, the finite element code will give excellent results. The case with $\eta=1.0$ and
 4 $\delta=0.02$ is more representative of what will be encountered with flow over and within a biphasic
 5 soft tissue.



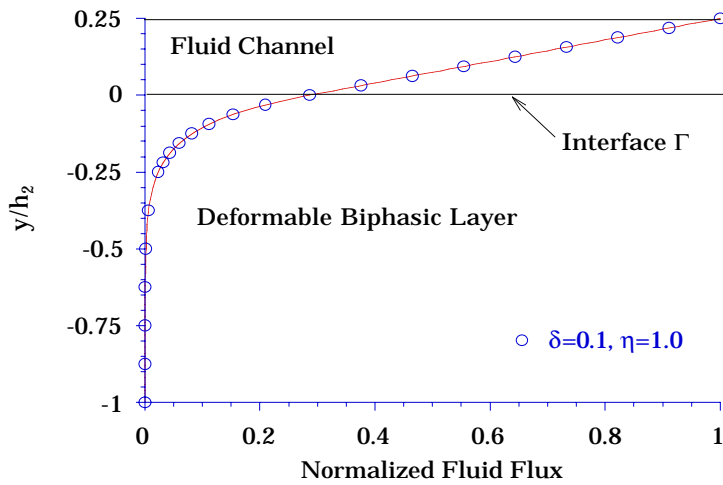
6
 7 Figure 4. Finite element solution (symbols) and analytical solution (line) of the fluid flux
 8 profile in the fluid channel and in the rigid porous layer (corresponding to Figure 2) for two
 9 different cases.

10 *Couette Flow over a Deformable Biphasic Layer*

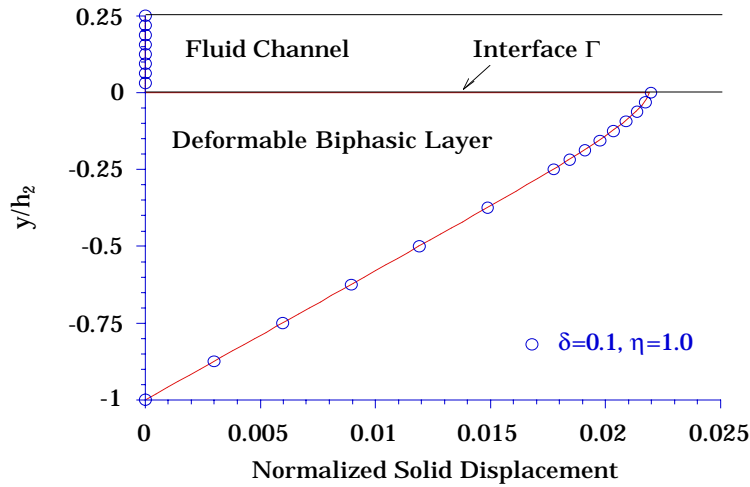
11 Using the boundary conditions derived by Hou, the analytical solution for Couette flow
 12 over a deformable biphasic medium has been developed². An example of a deformable biphasic
 13 medium would be articular cartilage. Typical values of δ for normal cartilage are in the range of
 14 $10^{-4} - 10^{-5}$. For such small values of δ , the amount of fluid flow in the biphasic layer will be very
 15 small for the present problem and the boundary layer that develops near the surface will be
 16 extremely narrow. As a result, the code will be validated using a value of $\delta=0.1$.

17 The schematic diagram of this flow problem is the same as that in Figure 2 with the rigid
 18 porous layer now being deformable. The single-phase viscous fluid is given a viscosity of

1 1.0Ns/m² (the viscosity of synovial fluid ¹³). For this example the porous deformable media will
 2 be modeled as a biphasic material with the material parameters chosen so that $\delta=0.1$ and $\eta=1.0$
 3 ($\lambda^s=0.1$ MPa, $\mu^s=0.3$ MPa, $\phi^s=0.2$, $\kappa=1.6\times 10^{-9}$ m⁴/Ns and $\mu^a=0.64$ Ns/m²). These properties are
 4 well within the norms for human articular cartilage ¹⁷. The boundary conditions for this problem
 5 are as before, with the exception that the solid velocities are now unknown on the left and right
 6 edges of the model. Since the solid is deformable and the height of the biphasic layer is greater
 7 than the fluid layer, the height of the biphasic layer is used in determining the length-to-height ratio
 8 of the geometry. A ratio of 10:1 for the length to biphasic layer height is used to produce the
 9 results in Figures 5 and 6.



10
 11 Figure 5. Finite element solution (symbols) and analytical solution (line) of the normalized
 12 fluid flux profile in the fluid channel and in porous medium with $\eta = 1.0$ and $\delta = 0.1$.



1
2 Figure 6. Finite element solution (symbols) and analytical solution (line) of the normalized
3 solid displacement profile of the deformable porous medium with $\eta = 1.0$ and $\delta = 0.1$.

4 Figures 5 and 6 show the results obtain for the Couette flow over a deformable porous-
5 permeable medium. Figure 5 shows the normalized velocity profile, $\phi^f v_x^f / V_0$, in the fluid channel
6 and in the biphasic medium. Figure 6 show the normalized solid displacement profile of the
7 deformable biphasic material. In this problem the normalized displacement is defined as the solid
8 displacement divided by the height of the deformable biphasic material, d^s/h_2 . The finite element
9 solution for both the fluid flux and solid displacement agree with the analytical solution.

10 SUMMARY AND CONCLUDING REMARKS

11 The fluid viscosity and interface boundary conditions have been added to the mixed-penalty
12 formulation of the linear biphasic theory for soft tissue and have been implemented into the finite
13 element code. The purpose of adding viscosity to the fluid phase is to be able to model a single-
14 phase, viscous fluid as a limiting case of a biphasic material. The addition of interface boundary
15 conditions allows us to model problems involving viscous incompressible fluids, elastic solids,
16 and biphasic materials, such as would be found in a diarthrodial joint. A volume-weighted mixture
17 velocity is introduced as a nodal degree of freedom for nodes on an interface. With proper

1 treatment of the constraints and of the assembly of elements, the interface kinematic boundary
2 conditions set forth by Hou ¹⁰ are satisfied exactly in the finite element solution.

3 The finite element code can now model any combination of interfaces involving viscous
4 incompressible fluids, elastic solids and biphasic materials. This is a first step toward modeling
5 the mechanisms of joint lubrication. Consideration should now be given to solving problems
6 representative of diarthrodial joint lubrication. For example, the problem of two opposing biphasic
7 layers separated by a layer of viscous incompressible synovial fluid is fundamental to the
8 understanding of joint lubrication. The finite element program can be used to solve this problem
9 up to the time when the biphasic tissues come into contact, after which the biphasic contact
10 approach of Donzelli and Spilker ⁶ must be used.

ACKNOWLEDGEMENTS

1

2

This work was supported by the National Science Foundation (ECS-9024235), the

3

National Institutes of Health (R01 AR42850) and the Surdna Foundation.

REFERENCES

- 1
- 2 ¹Armstrong, C.G. and V.C. Mow. Variations in the intrinsic mechanical properties of human
3 articular cartilage with age, degeneration, and water content. *J. Bone Jt. Surg.* 64A:88-94, 1982.
- 4 ²Ateshian, G.A. Biomechanics of diarthrodial joints: Application to the thumb carpometacarpal
5 joint. Ph.D. Thesis, New York, NY: Columbia University, 1991.
- 6 ³Ateshian, G.A., W.M. Lai, W.B. Zhu, and V.C. Mow. An asymptotic solution for the contact of
7 two biphasic cartilage layers. *J. Biomech.* 27:1347-1360, 1994.
- 8 ⁴Ateshian, G.A. and H. Wang. A theoretical solution for the frictionless rolling contact of
9 cylindrical biphasic articular cartilage layers. *J. Biomech.* 28:1341-1355, 1995.
- 10 ⁵Chan, B. A finite element formulation for interfaces between a biphasic hydrated soft tissue, a
11 viscous incompressible fluid and an elastic solid. M. S. Thesis, Troy, NY: Rensselaer Polytechnic
12 Institute, 1991, 62 pp.
- 13 ⁶Donzelli, P.S. and R.L. Spilker. A contact finite element formulation for biological soft hydrated
14 tissues. *Comp. Meth. Appl. Mech. Engng.* 153:63-79, 1998.
- 15 ⁷Freeman, M.A.R. and G. Meachim. Aging and degeneration. In: *Adult articular cartilage*, Edited
16 by M.A.R. Freeman. Kent, England: Pitman medical pub., 1979, 487-543 pp.
- 17 ⁸Hlavacek, M. The role of synovial fluid filtration by cartilage in lubrication of synovial joints--IV.
18 Squeeze-film lubrication: the central film thickness for normal and inflammatory synovial fluids for
19 axial symmetry under high loading conditions. *J. Biomech.* 28:1199-1205, 1995.
- 20 ⁹Hou, J., W.M. Lai, V.C. Mow, and M.H. Holmes. Interface conditions between fluids,
21 mixtures and solids: applications to biomechanics problems: ASME, 1989, 175-176 pp.

- 1 ¹⁰Hou, J.S., M.H. Holmes, W.M. Lai, and V.C. Mow. Boundary conditions at the cartilage-
2 synovial fluid interface for joint lubrication and theoretical verifications. *J. Biomech. Engng.*
3 111:78-87, 1989.
- 4 ¹¹Hughes, T.J.R. The Finite Element Method: Linear Static and Dynamic Analysis. Englewood
5 Cliffs: Prentice-Hall, Inc., 1987, 803 pp.
- 6 ¹²Jin, Z., D. Dowson, and J. Fisher. The effect of porosity of articular cartilage on the lubrication
7 of a normal human hip joint. *Proc. Instn Mech. Engrs.* 206:117-124, 1992.
- 8 ¹³Lai, W.M., S.C. Kuei, and V.C. Mow. Rheological equations for synovial fluids. *J. Biomech.*
9 *Engng.* 100:169-186, 1978.
- 10 ¹⁴Lai, W.M. and V.C. Mow. Drag-induced compression of articular cartilage during a permeation
11 experiment. *Biorheol.* 17:111-123, 1980.
- 12 ¹⁵Mankin, H.J., K.D. Brandt, and L.E. Shulman. Workshop on etiopathogenesis of
13 osteoarthritis. *J. Rheum.* 13:1130-1159, 1986.
- 14 ¹⁶Maxian, T.A. A six-node triangular element for the mixed-penalty finite element formulation of
15 the linear biphasic theory. Master of Science Thesis, Troy, NY: Rensselaer Polytechnic Institute,
16 1989.
- 17 ¹⁷Mow, V.C., S.C. Kuei, W.M. Lai, and C.G. Armstrong. Biphasic creep and stress relaxation
18 of articular cartilage in compression: theory and experiments. *J. Biomech. Engng.* 102:73-84,
19 1980.
- 20 ¹⁸Radin, E.L., I.L. Paul, and R.M. Rose. Role of mechanical factors in pathogenesis of primary
21 osteoarthritis. *Lancet.* 1:519-522, 1972.

- 1 ¹⁹Spilker, R.L. and T.A. Maxian. A mixed-penalty finite element formulation of the linear
2 biphasic theory for soft tissues. *Int. J. Num. Meth. in Engng.* 30:1063-1082, 1990.
- 3 ²⁰Spilker, R.L., J.-K. Suh, and V.C. Mow. A finite element formulation of the linear biphasic
4 representation of soft tissues. In: 1987 Biomechanics Symposium, Edited by D.L. Butler and P.A.
5 Torzilli. New York: ASME, 1987, 49-50 pp.
- 6 ²¹Spilker, R.L., J.-K. Suh, and V.C. Mow. A finite element formulation of the nonlinear biphasic
7 model for articular cartilage and hydrated soft tissues including strain-dependent permeability. In:
8 Computational Methods in Bioengineering, Edited by R.L. Spilker and B.R. Simon. New York:
9 ASME, 1988, 81-92 pp.
- 10 ²²Spilker, R.L., J.K. Suh, M.E. Vermilyea, and T.A. Maxian. Alternate hybrid, mixed, and
11 penalty finite element formulations for the biphasic model of soft hydrated tissues. In:
12 Biomechanics of Diarthrodial Joints, Edited by V.C. Mow, T.A. Ratcliffe, and S.Y.L. Woo. New
13 York: Springer-Verlag, 1990, 401-435 pp.
- 14 ²³Suh, J.K., R.L. Spilker, M.H. Holmes, and V.C. Mow. A nonlinear biphasic finite element
15 formulation for soft hydrated tissues under finite deformation. In: 1989 Advances in
16 Bioengineering, Edited by B. Rubinsky. New York: ASME, 1989, pp.
- 17 ²⁴Van Der Voet, A., N. Shrive, and N. Schachar. Numerical modelling of articular cartilage in
18 synovial joints - Poroelasticity and boundary conditions. In: Recent Advances in Computer
19 Methods in Biomechanics & Biomedical Engineering, Edited by J. Middleton, G. Pande, and K.
20 Williams. United Kingdom: Books & Journals International Ltd, 1993, pp.
- 21 ²⁵Vermilyea, M.E. and R.L. Spilker. A three-dimensional mixed-penalty finite element for the
22 biphasic model of soft hydrated tissues. In: 1990 Advances in Bioengineering, Edited by S.
23 Goldstein. New York: ASME, 1990, 211-214 pp.

FIGURE LEGENDS

1
2 Figure 1. Portion of a finite element mesh at an interface between two dissimilar materials.
3 An interface element is one which contains at least one interface node.
4

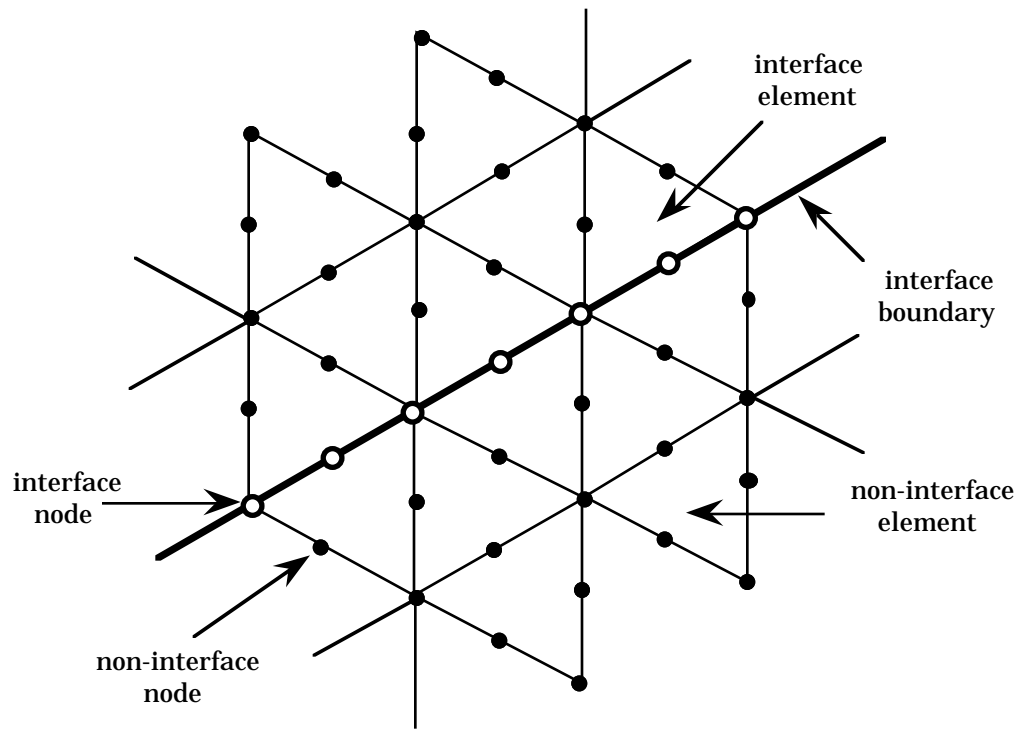
5 Figure 2. Schematic diagram of Couette flow over a porous-permeable layer. The finite
6 element model will contain only the fluid channel and rigid, porous layer. Solid velocity is
7 set to zero at all boundaries of the model. Fluid velocity is prescribed to V_0 at the top of the
8 fluid channel, and zero at the bottom of the porous layer, and is unknown at the left and
9 right edges.
10

11 Figure 3. Finite element solution (symbols) and analytical solution (line) of the fluid flux
12 profile in the fluid channel and in the rigid porous layer (corresponding to Figure 2) with η
13 = 1 and $\delta = 0.1$.
14

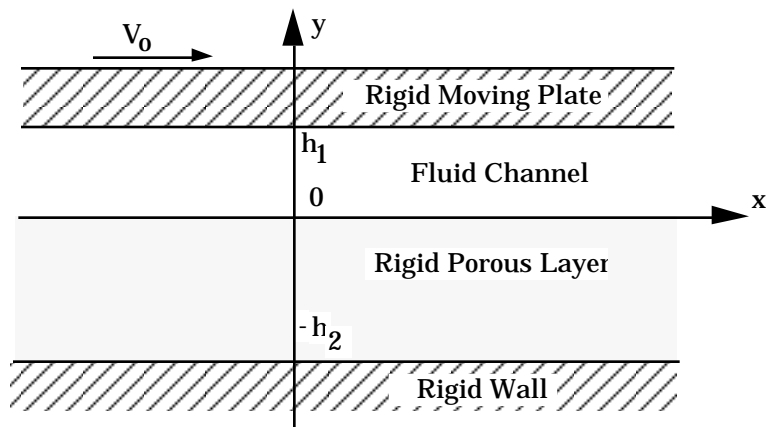
15 Figure 4. Finite element solution (symbols) and analytical solution (line) of the fluid flux
16 profile in the fluid channel and in the rigid porous layer (corresponding to Figure 2) for two
17 different cases.
18

19 Figure 5. Finite element solution (symbols) and analytical solution (line) of the normalized
20 fluid flux profile in the fluid channel and in porous medium with $\eta = 1.0$ and $\delta = 0.1$.
21

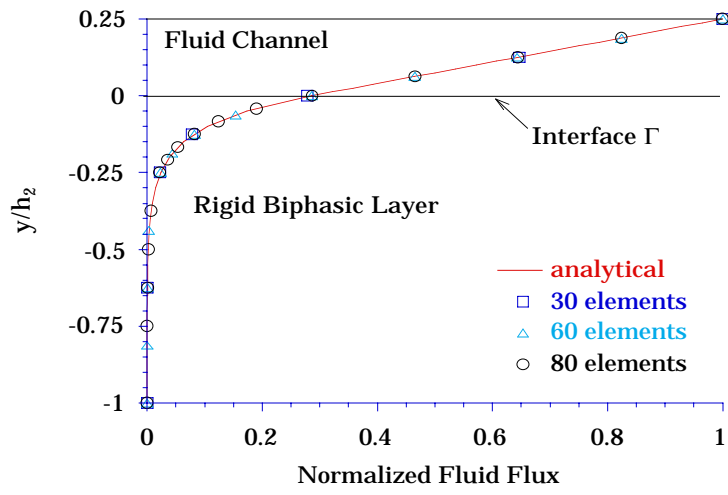
22 Figure 6. Finite element solution (symbols) and analytical solution (line) of the normalized
23 solid displacement profile of the deformable porous medium with $\eta = 1.0$ and $\delta = 0.1$.
24



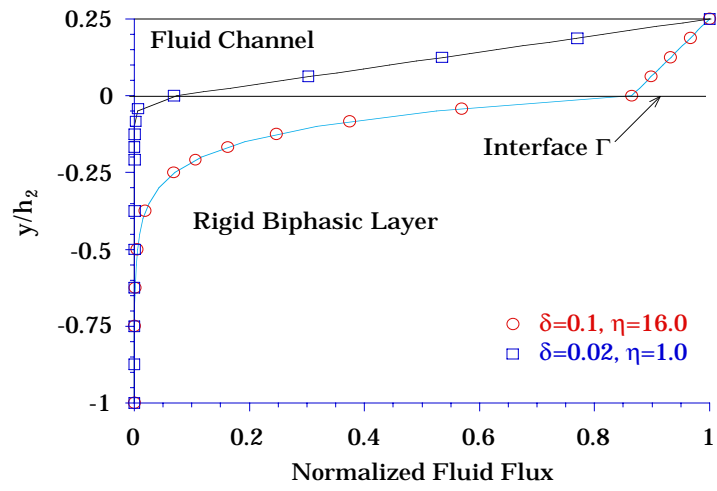
1



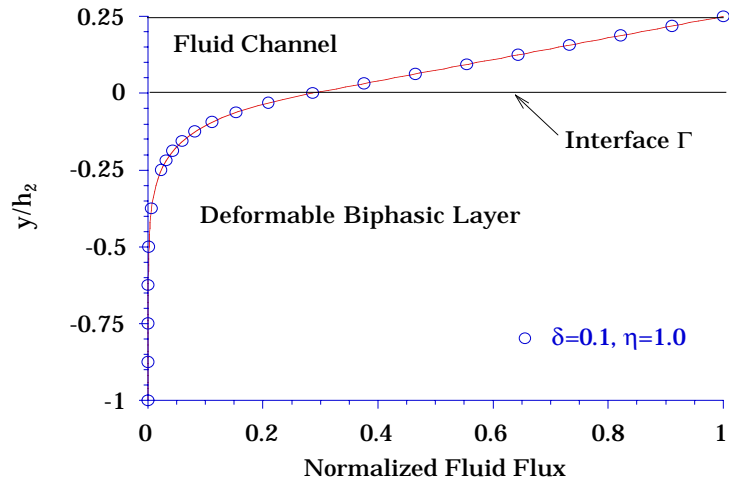
1



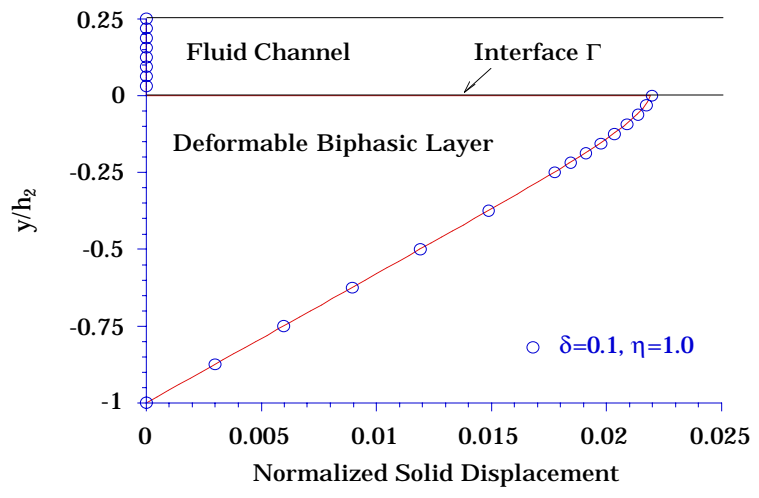
1



1



1



1

2